

## A NEAR INPUT-OUTPUT LINEARIZING FORCE TRACKING CONTROLLER FOR AN ELECTROHYDRAULIC ACTUATOR

### Beshahwired Ayalew

The Pennsylvania State University  
The Pennsylvania Transportation Institute  
206 Transportation Research Building  
University Park, PA16802, USA  
Email: [beshah@psu.edu](mailto:beshah@psu.edu)  
Phone: (814)863-8057  
Fax: (814)865-3039

### Bohdan T. Kulakowski

The Pennsylvania State University  
The Pennsylvania Transportation Institute  
201 Transportation Research Building  
University Park, PA16802, USA  
Email: [bt1@psu.edu](mailto:bt1@psu.edu)  
Phone: (814)863-1893  
Fax: (814)865-3039

### Kathryn W. Jablokow

Penn State Great Valley  
30 E. Swedesford Road  
Malvern, PA 19355  
Email: [kwl3@qv.psu.edu](mailto:kwl3@qv.psu.edu)  
Phone: (610)648-3372  
Fax: (610)648-3377

### ABSTRACT

Under simple practical assumptions, the theory of feedback linearization can be applied to a physical model of an electrohydraulic rectilinear actuator. This paper presents the derivation of a near input-output (IO) linearizing force tracking controller and its experimental implementation on a fatigue testing electrohydraulic actuator. Comparisons are conducted against a linear state feedback with integral controller and a standard PID controller. It is shown that, within the limits of investigated system bandwidth and smoothness restrictions of the desired force trajectory, the near IO linearizing controller has better tracking properties. It is also noted that a sliding mode controller can be interpreted as a robust version of the near IO linearizing controller. Experiments are conducted to investigate the robustness of the controlled system to the parameters of the near IO linearizing controller.

Key Words: feedback linearization, input-output linearization, pressure tracking, force tracking, electrohydraulic actuator, state feedback with integral control, fatigue testing

### INTRODUCTION

Electrohydraulic actuators constitute important force generation elements in a variety of industrial applications. Their high load stiffness, high level of self cooling, and high power-to-weight ratio make them better choices than electromechanical actuators in many applications. However, electrohydraulic actuators exhibit significant nonlinearities in their dynamics. In order to obtain satisfactory performance in the presence of these nonlinearities, more elaborate control techniques than the ubiquitous PID loops may be necessary.

The literature offers a wide variety of methods for improving the position and force tracking performance of electrohydraulic actuators. These include variants of linear state

feedback [10], adaptive control [1, 10, 17, 21, 26], variable structure control [13, 15] and Lyapunov-based controller designs [1, 9, 18, 20, 21]. Each approach has its own strengths and limitations, which are outlined in the respective listed references. In this work, the focus is to present an evaluation of a near feedback linearization approach to force tracking control via experiments on an electrohydraulic actuator in a fatigue testing application.

Feedback linearization involves the transformation of a nonlinear system to a linear one via state feedback and input transformation. A formal theory of feedback linearization is detailed in the texts by Slotine and Li [19] and Khalil [11]. The method applies to systems whose model structure allows such transformations to be performed. As will be shown in this paper, under some specific assumptions, the model of an electrohydraulic actuator can be put in a form that approaches a partial feedback linearizable or input-output (IO) linearizable form.

Perhaps the earliest study on the application of feedback linearization to electrohydraulic actuators was that of Axelson and Kumar [3] in 1988. Their work presented the derivation of the control law emphasizing the nonlinearity for valve orifice flow only. No simulation or experimental results were published. Hahn, et al. [8] derived a more detailed controller for the position tracking case, including the major nonlinearities arising from valve flow and nonlinear hydraulic compliance. They presented limited results from implementations in simulation only. Vossoughi and Donath [24] presented an analysis and derivation of a feedback linearizing controller for a velocity tracking in robotic application of asymmetric actuators. Del Re and Isidori [6] discussed the application of feedback linearization to approximate models obtained by replacing the original nonlinear model with linear-bilinear

cascade model interconnections. Their application was the control of the rotational velocity output of a hydrostatic transmission.

In this work, the derivation and application of near input-output linearizing force tracking controllers are discussed. Emphasis is placed on the experimental investigation of robustness to model parameter uncertainty. The rest of the paper is organized as follows. We first describe the system under consideration and then outline the model of the actuator. The control law derivation is detailed followed by a discussion of experimental results. Finally, the conclusions of the paper are presented.

## NOMENCLATURE

$A_F$	amplitude of force step magnitude in Eq (39)
$A_b, A_t$	piston areas for the bottom and top chambers, respectively
$C_L$	leakage coefficient used in controller
$C_{Lb,t}$	leakage coefficients computed from the separate equations (44) and (45)
$C_v$	valve coefficient used in controller
$C_{v,i}; i=1,2,3,4$	valve coefficient referred to each port
$e_F$	pressure force tracking error
$f$	arbitrary scalar or vector function
$f_F$	nonlinear feedback term given by Eq (16)
$F_f$	friction force on piston
$F_L$	load force or specimen reaction on piston
$F_{L,d}$	desired or reference load force trajectory
$F_p$	fluid pressure force on piston
$F_{p,d}$	desired or reference pressure force trajectory
$f_{pL}$	nonlinear feedback term given by Eq (31)
$g_F$	nonlinear feedback term given by Eq (17)
$g_{pL}$	nonlinear feedback term given by Eq (32)
$G_V$	static gain of the valve
$i, k$	indexing integers
$i_v$	servo valve current
$\bar{i}_v$	net servo valve current
$i_{v,off}$	offset current to account for abrasion wear and lap conditions
$k_l$	positive constant gain in closed loop system, Eq (26)
$k_o$	constant positive gain of closed loop system, Eq (21)
$K_{v,i}; i=1,2,3,4$	valve coefficients defined with spool position
$K_s$	linear specimen stiffness
$m_p$	lumped mass of piston, fixture and oil mass in cylinder
$p_b, p_t$	pressure in the bottom and top cylinder chambers, respectively
$p_L$	load or differential pressure ( $p_L=p_b-p_t$ )
$p_R$	return pressure at servo valve
$p_S$	supply pressure at servo valve
$q_b, q_t$	flow to the bottom and from the top cylinder chambers, respectively

$q_{e,b}$	external leakage from the bottom and top chambers, respectively
$q_{e,t}$	respectively
$q_i$	internal leakage in cylinder
$t, T, t_o$	time, smoothing factor, and step time, respectively, used in Eq (39)
$u_1, u_2, u_3, u_4$	underlap or overlap lengths for servovalve spool
$V_b, V_t$	bottom and top cylinder chamber volumes, respectively
$v_p$	piston velocity
$x$	dummy variable
$x_p$	piston position
$x_v$	servovalve spool displacement
$x_{v,off}$	offset spool displacement
$\beta_b, \beta_t$	estimated bulk modulus for bottom and top chambers, respectively
$\beta_e$	effective bulk modulus

## MODEL OF TEST SYSTEM

Figure 1 shows the schematic of the hydraulic system considered for this study. The servovalve is a 5 gpm (19 lpm) two-stage servovalve, which employs a torque motor-driven, double nozzle-flapper first stage and a main spool output stage. The servovalve is close-coupled with a 10 kN, 102 mm-stroke symmetric actuator, which is mounted on a load frame. Two pressure transducers are used for sensing the pressures at the output ports of the servovalve. An LVDT is mounted on the actuator piston for position measurement.

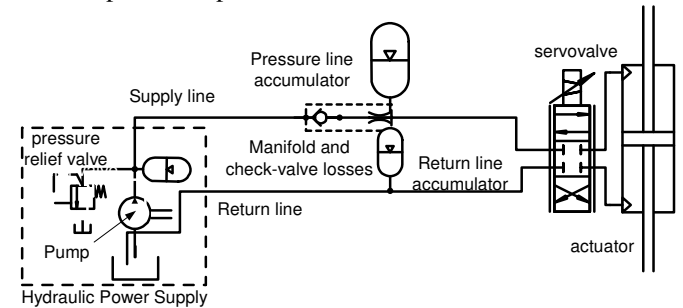


**Figure 1 Simplified schematic of the test system.**

The Hydraulic Power Supply (HPS) unit, including its heat exchanger and drive units, is housed separately and is connected to the service manifold block via 3.048 m-long SAE-100R2 hoses. The manifold block contains an in-line check valve and a filter element on the supply line; it is equipped with a control manifold circuitry to permit selection of high- and low-pressure operating modes, low-pressure level adjustment, slow pressure turn-on and turn-off, and fast pressure unloading. The supply and return accumulators are mounted directly on the manifold, which is in turn connected to the servovalve using 3.048 m-long SAE-100R2 hoses. During normal fatigue testing operations, the manifold circuitry allows flow at full system pressure. A study of the complete system model, including the transmission hoses, the manifold and the accumulators, is published by the authors in [5]. It is shown there that the ideal configuration would close-couple the accumulators to the servovalve (remove the second set of hoses between the accumulators and the servovalve), thereby effectively exploiting the accumulators in eliminating pressure transients at the supply and return ports of the servovalve. Therefore, for the

sole purpose of deriving the nonlinear control laws, it will be assumed that the supply and return pressures at the ports of the servovalve can be considered constant.

Physical models of electrohydraulic servo-actuators are quite widely available in the literature [7, 10, 12, 14, 20, 22, 23, 25]. The model presented here is adapted to apply to a four-way servovalve, close-coupled with a double-ended piston actuator. Figure 2 shows a double-ended translational piston actuator with hydraulic flow rates,  $q_t$  from the top chamber and,  $q_b$  to the bottom chamber of the cylinder. Leakage flow between the two chambers is either internal ( $q_i$ ) between the two chambers or external from the top chamber ( $q_{e,t}$ ) and from the bottom chamber ( $q_{e,b}$ ).  $A_t$  and  $A_b$  represent the effective piston areas of the top and bottom face, respectively.  $V_t$  and  $V_b$  are the volumes of oil in the top and bottom chambers of the cylinder, respectively, corresponding to the center position ( $x_p=0$ ) of the piston. These volumes are also assumed to include the respective volumes of oil in the pipelines between the close-coupled servovalve and actuator, as well as the small volumes in the servovalve itself.

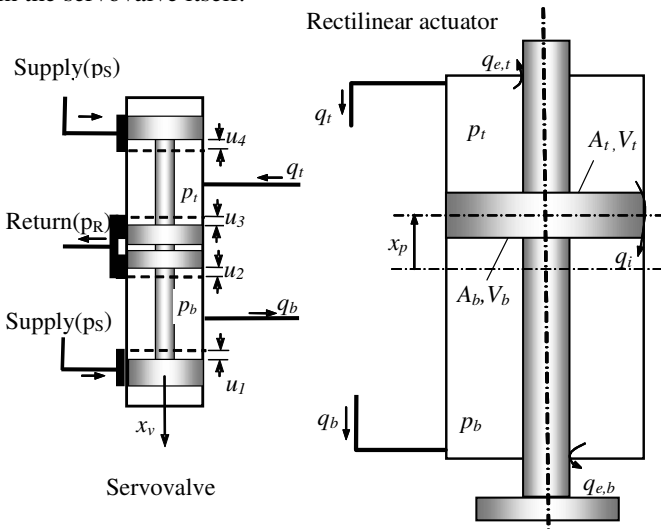


**Figure 2 Schematic of rectilinear servovalve and actuator**

It is assumed here that the pressure dynamics in the lines between the servovalve and the actuator are negligible due to the close-coupling. Furthermore, even for a long-stroke actuator used in a flight simulator application, where close-coupled mounting is not feasible, Van Schothorst [22] has shown that the pressure dynamics in the actuator chambers need not be modeled using distributed parameter models. It is therefore assumed that the pressure is uniform in each cylinder chamber.

Starting with the continuity equation and introducing the state equation with the effective oil bulk modulus for the cylinder chambers, it can be shown that the pressure dynamics are given by (see, for example [12])

$$\frac{dp_b}{dt} = \frac{\beta_e}{V_b + A_b x_p} (q_b - A_b \dot{x}_p + q_i - q_{e,b}) \quad (1)$$

$$\frac{dp_t}{dt} = \frac{\beta_e}{V_t - A_t x_p} (-q_t + A_t \dot{x}_p - q_i - q_{e,t}) \quad (2)$$

These equations show that the hydraulic capacitance, and hence the pressure evolution in the two chambers, depends on the piston position. The leakage flows,  $q_{e,b}$ , and  $q_{e,t}$ , are

considered negligible. The internal leakage past the piston seals is assumed here to be laminar, with a leakage coefficient,  $C_L$ , as follows:

$$q_i = C_L (p_t - p_b) \quad (3)$$

The predominantly turbulent flows through the sharp-edged control orifices of a spool valve to and from the two sides of the cylinder chambers are modeled by nonlinear expressions [10, 12, 14]. Assuming positive flow directions, as shown in Fig. 2, these flows are given by:

$$q_b = K_{v,1} sg(x_v + u_1) \operatorname{sgn}(p_S - p_b) \sqrt{|p_S - p_b|} - K_{v,2} sg(-x_v + u_2) \operatorname{sgn}(p_b - p_R) \sqrt{|p_b - p_R|} \quad (4)$$

$$q_t = K_{v,3} sg(x_v + u_3) \operatorname{sgn}(p_t - p_R) \sqrt{|p_t - p_R|} - K_{v,4} sg(-x_v + u_4) \operatorname{sgn}(p_S - p_t) \sqrt{|p_S - p_t|} \quad (5)$$

where the function,  $sg(x)$ , is defined by:

$$sg(x) = \begin{cases} x, & x \geq 0 \\ 0, & x < 0 \end{cases} \quad (6)$$

The parameters,  $u_1, u_2, u_3, u_4$ , are included to account for valve spool lap conditions as shown in Fig. 2. Negative values represent overlap, while positive values represent underlap. Since the valve discharge coefficients, which largely determine the valve coefficients  $K_{v,i}, i=1,2,3,4$ , change with service life, the “valve coefficients” can and should be estimated from simple experiments (see Appendix).

The state equations governing piston motion are derived considering the loading model for the actuator. For the test system, the actuator cylinder is rigidly mounted on a load frame, as shown in Fig. 3. The load frame is used as an inertial frame.

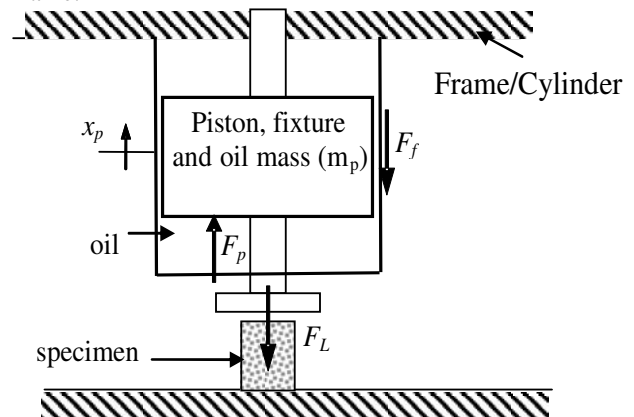


**Figure 3 Forces on the actuator piston**

The upward force on the actuator piston due to the oil pressure in the two cylinder chambers is given by:

$$F_p = A_b p_b - A_t p_t \quad (7)$$

The friction force on the piston in the cylinder is denoted by  $F_f$ , and the external loadings, including specimen stiffness and damping forces, are lumped together in  $F_L$ . In Fig. 3,  $F_L$  is considered tensile positive. The equations of motion are derived by applying Newton's Second Law:

$$\dot{x}_p = v_p \quad (8)$$

$$\dot{v}_p = \frac{1}{m_p} [A_b p_b - A_t p_t - F_L - F_f - m_p g] \quad (9)$$

Equations (1), (2), (8) and (9), with  $q_b$  and  $q_t$  given by Eqs (4) and (5), constitute the state space model for the servovalve and loaded actuator subsystem under consideration. These equations also contain the major nonlinearities in the system, which are the variable hydraulic capacitance and the square root flow rate versus pressure drop relations. Nonlinearity is also introduced in Eq (9) by the nonlinear friction force, which includes Coulomb, static, and viscous components [5].

## CONTROL LAW DERIVATION

### Basic Assumptions

For the control law derivation in this paper, the servovalve is considered to be critically centered with symmetric and matched orifices. That is, the underlap/overlap lengths are neglected. Instead, an offset value of the valve position can be estimated during calibration to take into account any abrasion-induced null offsets [12]. Also, the valve spool dynamics are ignored. This implies that the valve spool position is assumed to be related to the servovalve current with a static gain  $G_v$ , as given by:

$$\bar{i}_v = G_v \bar{x}_v \quad (10)$$

where,  $\bar{i}_v = i_v - i_{voff}$ , and  $\bar{x}_v = x_v - x_{voff}$ , with  $i_{voff}$  and  $x_{voff}$  representing the current offset and valve spool position offset, respectively.

With these assumptions, either the servovalve current or the valve spool position can be considered as the control variable for analysis. Since the valve spool position measurement is not available for the test system under consideration, and also to maintain consistency with the true control input, only the servovalve current is used as the control variable in this paper. The flow rates to and from the cylinder chambers are then rewritten as follows:

$$q_b = C_{v,1} s g(\bar{i}_v) \text{sign}(p_S - p_b) \sqrt{|p_S - p_b|} - C_{v,2} s g(-\bar{i}_v) \text{sign}(p_b - p_R) \sqrt{|p_b - p_R|} \quad (11)$$

$$q_t = C_{v,3} s g(\bar{i}_v) \text{sign}(p_t - p_R) \sqrt{|p_t - p_R|} - C_{v,4} s g(-\bar{i}_v) \text{sign}(p_S - p_t) \sqrt{|p_S - p_t|} \quad (12)$$

where the new valve coefficients referenced to the current are given by:

$$C_{v,i} = G_v K_{v,i} \quad i = 1, 2, 3, 4 \quad (13)$$

The form of the flow rate equations given by Eqs (11) and (12) make it possible to estimate the actual valve coefficients from experimental data as described in the Appendix.

### Pressure Force Tracking Control

Taking the derivative of the piston force in Eq (7), and using Eqs (1) and (2), it can be shown that:

$$\dot{F}_p = -\dot{x}_p \beta_e \left( \frac{A_b^2}{V_b + A_b x_p} + \frac{A_t^2}{V_t - A_t x_p} \right) + \frac{A_b \beta_e}{V_b + A_b x_p} (q_b + q_i) + \frac{A_t \beta_e}{V_t - A_t x_p} (q_t + q_i) \quad (14)$$

where the external leakages,  $q_{b,e}$  and  $q_{t,e}$ , are neglected. Using Eqs (13) and (14) for  $q_b$  and  $q_t$ , and regrouping variables, Eq (14) can be rewritten as follows:

$$\dot{F}_p = f_F(x_p, \dot{x}_p, p_b, p_t) + g_F(x_p, p_b, p_t, \text{sgn}(\bar{i}_v)) \bar{i}_v \quad (15)$$

where the nonlinear functions,  $f_F$  and  $g_F$ , are, respectively:

$$f_F(x_p, \dot{x}_p, p_b, p_t) = -\dot{x}_p \beta_e \left( \frac{A_b^2}{V_b + A_b x_p} + \frac{A_t^2}{V_t - A_t x_p} \right) + \frac{A_b \beta_e C_L (p_t - p_b)}{V_b + A_b x_p} + \frac{A_t \beta_e C_L (p_t - p_b)}{V_t - A_t x_p} \quad (16)$$

$$g_F(x_p, p_b, p_t, \text{sgn}(i_v)) = \begin{cases} \frac{A_b \beta_e C_v}{V_b + A_b x_p} \text{sgn}(p_S - p_b) \sqrt{|p_S - p_b|} \\ + \frac{A_t \beta_e C_v}{V_t - A_t x_p} \text{sgn}(p_t - p_R) \sqrt{|p_t - p_R|} & \text{for } \bar{i}_v \geq 0 \\ \frac{A_b \beta_e C_v}{V_b + A_b x_p} \text{sgn}(p_b - p_R) \sqrt{|p_b - p_R|} \\ + \frac{A_t \beta_e C_v}{V_t - A_t x_p} \text{sgn}(p_S - p_t) \sqrt{|p_S - p_t|} & \text{for } \bar{i}_v < 0 \end{cases} \quad (17)$$

Equation (15), with  $f_F$  and  $g_F$  defined by Eqs (16) and (17), respectively, contains all the major modeled nonlinearities in the hydraulic system that arise from fluid compliance and turbulent orifice flow. Also, the derivative of the output piston force,  $F_p$ , is seen to be only piecewise linear in the control input ( $\bar{i}_v$ ). This suggests that an input-output linearization with a relative degree of one can be performed in the respective domains ( $\bar{i}_v \geq 0$  and  $\bar{i}_v < 0$ ) [11, 19]. Furthermore, the nonlinearities in the piston force dynamics given by Eq (15) can be cancelled by choosing the piecewise IO linearizing control input:

$$\bar{i}_v = \frac{1}{g_F(x_p, p_b, p_t, \text{sgn}(\bar{i}_v))} (v - f_F(x_p, \dot{x}_p, p_b, p_t)) \quad (18)$$

where  $v$  is a new (transformed) control input. The piston force dynamics given by Eq (15) reduce to:

$$\dot{F}_p = v \quad (19)$$

This is a simple linear integrator, which can easily be stabilized by state feedback. Exponentially convergent tracking of a

desired differentiable piston force profile ( $F_{p,d}$ ) can be achieved by choosing  $v$  as follows:

$$v = \dot{F}_{p,d} - k_o(F_p - F_{p,d}) \quad (20)$$

The force tracking error dynamics are given by:

$$e_F + k_o e_F = 0 \quad (21)$$

where  $e_F$  is the force tracking error,  $e_F = F_p - F_{p,d}$ .

In summary, the control input of Eq (18), with  $v$  given by Eq (20) and a proper choice of  $k_o > 0$ , can give a desired degree of exponential force tracking performance, regardless of the nonlinearities in Eq (15), provided the internal dynamics are stable. In terms of the force tracking error, the control current is given by:

$$\bar{i}_v = \frac{1}{g_F(x_p, p_b, p_t, \text{sgn}(\bar{i}_v))} (\dot{F}_{p,d} - k_o e_F - f_F(x_p, \dot{x}_p, p_b, p_t)) \quad (22)$$

It is important to note that Eq (22) cannot be solved "as is", since it contains the control variable,  $\bar{i}_v$ , on both sides of an equation involving the sgn function. A practical solution to this problem becomes evident when considering the digital implementation of the piecewise IO linearizing controller. The sign of the value of  $\bar{i}_v$  at the previous time step can be used to compute the value of  $\bar{i}_v$  at the current time step, if it can be supposed that the current does not change signs at a rate faster than the sampling rate. However, it is difficult to analytically prove that this approach does not lead to control chatter. This chatter problem has not been reported previously in the literature that discusses feedback linearization for hydraulic drives [6, 8, 24]. In addition, the problem has not been experienced during any of the experiments performed for this paper.

The name near input-output (near IO) linearization is adopted in this paper to make the explicit distinction that the present controller is not a true IO linearizing controller in the traditional sense, but it is very close. It should be noted that the piecewise IO linearization gave a system of relative degree one in each domain. That is, only one differentiation of the output was needed before the input appeared. The external dynamics are given by Eq (21). It remains to evaluate the stability of the internal dynamics of degree 3, which involve system states that are rendered "unobservable" during the piecewise IO linearization. An investigation of the internal dynamics is better handled by introducing the concept of load pressure, which is done next.

### Load Force Tracking Control

This section is included to highlight aspects of the IO linearization approach to the control of the net force applied to the specimen, which is referred to in this paper as the load force ( $F_L$ ). This is given by:

$$F_L = F_p - F_f - m_p(g + \ddot{x}_p) \quad (23)$$

Differentiating Eq (23) and using Eq (15), we obtain:

$$\dot{F}_L = f_F(x_p, \dot{x}_p, p_b, p_t) - \dot{F}_f - m_p(\ddot{x}_p) + g_F(x_p, p_b, p_t, \text{sgn}(\bar{i}_v))\bar{i}_v \quad (24)$$

Proceeding as above, the near IO linearizing controller with this definition of system output can be shown to be:

$$\bar{i}_v = \frac{1}{g_F(x_p, p_b, p_t, \text{sgn}(\bar{i}_v))} (\dot{F}_{L,d} - k_l(F_L - F_{L,d}) - f_F(x_p, \dot{x}_p, p_b, p_t) - \dot{F}_f - m_p(\ddot{x}_p)) \quad (25)$$

Here, the gain  $k_l$  is chosen to stabilize the closed-loop force tracking error dynamics, which is given by:

$$(F_L - \dot{F}_{L,d}) + k_l(F_L - F_{L,d}) = 0 \quad (26)$$

Note that the load force tracking controller given by Eq (25) needs additional variables for feedback, as compared to the one given in Eq (22). Namely, the controller requires feedback of the derivatives of the friction force and the inertia force, as well as a feedback of the load force (from a load cell). It is particularly important that an accurate and differentiable approximation of the friction force be found. While these problems can be approximated in various ways, they are not pursued any further in this paper.

### Descriptions using the load pressure

The expression for the pressure force controller can be rewritten by introducing the so-called load pressure or differential pressure:

$$p_L = p_b - p_t \quad (27)$$

and assuming further that the valve ports are matched and symmetrical ( $C_{v,1} = C_{v,2} = C_{v,3} = C_{v,4}$ ). In this case, it can be shown that [14]:

$$p_b = \frac{1}{2}(p_S + p_R + p_L) \quad (28)$$

$$p_t = \frac{1}{2}(p_S + p_R - p_L) \quad (29)$$

With these expressions, the state equations for the chamber pressures can be replaced with a single state equation for the load pressure, thereby reducing the order of the modeled system from four to three. This new state equation is given by:

$$\dot{p}_L = f_{p_L}(x_p, \dot{x}_p, p_L) + g_{p_L}(x_p, p_L, \text{sgn}(\bar{i}_v))\bar{i}_v \quad (30)$$

where

$$f_{p_L}(x_p, \dot{x}_p, p_L) = -\beta_e \dot{x}_p \left( \frac{A_b}{V_b + A_b x_p} + \frac{A_t}{V_t - A_t x_p} \right) - \beta_e C_L p_L \left( \frac{1}{V_b + A_b x_p} + \frac{1}{V_t - A_t x_p} \right) \quad (31)$$

$$g_{p_L}(x_p, p_L, \text{sgn}(\bar{i}_v)) = \beta_e C_v \sqrt{\left( \frac{p_S - p_R}{2} \right)} \times \sqrt{1 - \frac{p_L}{p_S - p_R} \text{sgn}(\bar{i}_v)} \times \left( \frac{1}{V_b + A_b x_p} + \frac{1}{V_t - A_t x_p} \right) \quad (32)$$

Recall that the other two state equations are given by Eqs (8) and (9).

For a symmetric actuator ( $A_b=A_r=A_p$ ), the pressure force dynamics are given by slightly simpler expressions, namely:

$$\dot{\hat{F}}_p = A_p \dot{p}_L = f_F(x_p, \dot{x}_p) + g_F(x_p, p_L, \text{sgn}(\bar{i}_v))\bar{i}_v \quad (33)$$

where,

$$f_F(x_p, \dot{x}_p) = A_p f_{pL}(x_p, \dot{x}_p) \quad (34)$$

$$g_F(x_p, p_L, \text{sgn}(\bar{i}_v)) = A_p g_{pL}(x_p, p_L, \text{sgn}(\bar{i}_v)) \quad (35)$$

The rest of the expressions leading to the near IO linearizing controller are the same as the general case given above. Only the expressions for the terms  $f_F$  and  $g_F$  need to be replaced with those given in Eqs (36) and (37). It should be recognized that the IO linearization achieved is of relative degree one. Second-order internal dynamics remain, the stability of which is straightforward to analyze.

It should also be noted that the pressure force control problem and the differential or load pressure control problem differ only by a factor of the piston area. Therefore, the force control conclusions discussed in this paper apply equally well to the differential pressure control case.

### Robust Pressure Force Tracking: Sliding Control

It turns out that the form of the near IO linearizing controller for pressure force tracking can be easily re-considered from a sliding control point of view and thereby formally address the issue of robustness. Here, we present the main results from sliding mode control. The reader is referred to [19] for a discussion of sliding mode control and ref[2, 4] for the derivation and experimental validation of the results briefly outlined here. Dropping the arguments of, and replacing the function  $f_F$  and  $g_F$  by their estimates  $\hat{f}_F$  and  $\hat{g}_F$ , respectively, the resulting (continuous version) sliding mode controller is:

$$\bar{i}_v = \frac{1}{\hat{g}_F} (\dot{\hat{F}}_{p,d} - K \text{sat}(S / \Phi) - \hat{f}_F) \quad (36)$$

where the  $\Phi$  is the boundary layer thickness and  $S$  is sliding surface variable defined by

$$S = F_p - F_{p,d} \quad (37)$$

and  $K$  is the gain, which should be chosen to satisfy

$$K \geq \delta g_F (\eta + \delta \hat{f}_F) + |1 - \delta g_F| \left| \dot{\hat{F}}_{p,d} - \hat{f}_F \right| \quad (38)$$

where the terms on the right contain uncertainty bounds on the functions  $f_F$  and  $g_F$ . Note that within the boundary layer ( $S \leq \Phi$ ), the sliding mode controller given by Eq (36) is identical to the near IO linearizing controller given by Eq (22).

## EXPERIMENTS

The experiments in this section consider a realistic loading on a fatigue test specimen. The piston is constrained instead with a neoprene rubber specimen so that large force magnitudes can be absorbed. Since the nonlinear controller uses the derivative of the reference (desired) force trajectory, smooth desired force trajectories need to be used. In particular, to compare step response, it was found necessary to approximate

the Heaviside step function (which has sharp corners, and hence is non-differentiable) by the following differentiable function involving the hyperbolic tangent function:

$$F_d = A_F \tanh\left(\frac{t - t_o}{T}\right) \quad (39)$$

Here,  $A_F$  is the size of the step,  $t_o$  is the time at which the step is applied, and  $T$  is a parameter that defines the ‘‘sharpness’’ of the corners of the approximated step. In the limit, as  $T \rightarrow 0$ , the function approaches the Heaviside step function with sharp corners.

As mentioned before, the experimental system uses an LVDT for position measurement, which is low-pass filtered with a cut-off frequency of 30Hz before differentiating the signal to obtain the piston velocity. The differential pressure feedback from two chamber pressure transducers was used to compute the pressure force output. The sampling rate was set at 1kHz.

### Nominal Performance of the Nonlinear Controller

The nominal nonlinear controller is the controller as derived above (Eq (22)) employing the nominal model parameters for the effective bulk modulus ( $\beta_e$ ), the valve coefficient ( $C_v$ ), the leakage coefficient  $C_L$ , and the supply ( $p_s$ ) and return ( $p_R$ ) pressures at the servovalve. The first three model parameters can be estimated using simple experiments, as outlined in the Appendix. The last two are known to change dynamically with the dynamics of supply and return hoses and accumulators [5]. However, the frequency ranges considered here are well below the influence of these line dynamics, thereby limiting the bandwidth of the experiments.

For a comparison of the performance of the nonlinear controller with standard linear controllers, a well-tuned PID controller, as well a linear state feedback with integral (LSFI) controller[16] are considered. The latter uses feedback of the same states as the nonlinear controller. To design the LSFI controller, a local linearization (Jacobian Linearization) of the nonlinear system model described earlier was obtained with the piston at a nominal position corresponding to the experiments. Since the actual plant is nonlinear, some tuning of the gains was found necessary.

Figure 4 shows a basic comparison of the nonlinear controller (NLC) with a gain setting of  $k_o=750 \text{ s}^{-1}$ , well-tuned PID and LSFI controller, for a smooth force reference trajectory defined by Eq (39) with  $T=0.02$  sec. It is stressed here that the gains finally used for the PID and LSFI controllers are those giving satisfactory experimental response with no steady state error or oscillations. It should be recognized that, for example, it is possible to reduce the overshoot with the PID controller by reducing the I-gain of the PID while allowing steady state error.

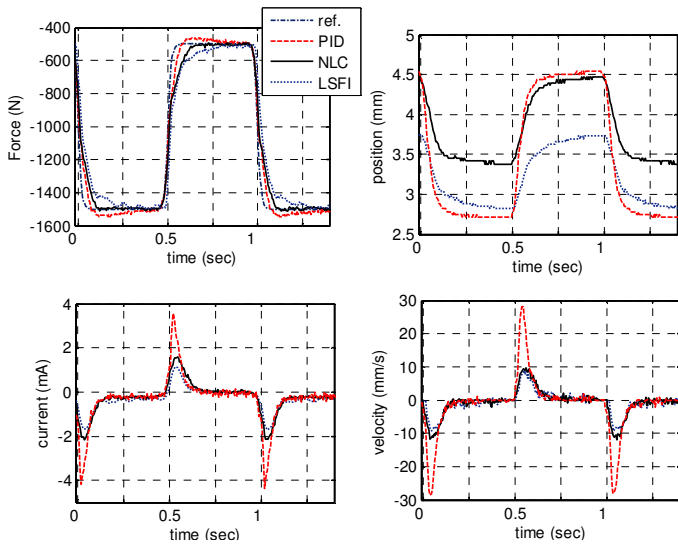


**Figure 4 Experimental comparison of the nominal nonlinear controller with linear controllers**

It can be seen from Fig. 4 that due to the overshoot in the force response with the PID controller, the specimen was compressed the most (piston travel was the highest) and the magnitude of the control current required was the highest in the PID control case. The linear state feedback with integral (LSFI) controller resulted in a sluggish force response with the least piston travel. The performance of the nominal nonlinear controller was the best of the three considering the rise time and settling time, absence of overshoot in the force response as well as the magnitude of the control current.

The performance of the nominal near IO linearizing controller can be tuned further by using the gain  $k_o$ . Figure 5 shows responses as the gain  $k_o$ , was changed over a range of values.

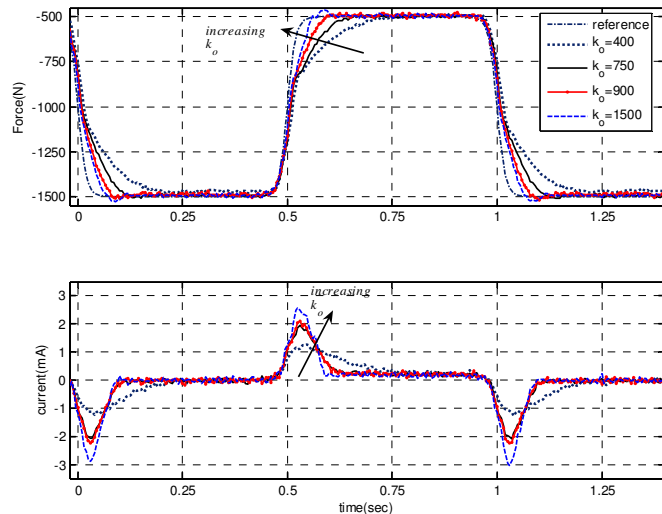


**Figure 5 Tuning the nominal nonlinear controller with  $k_o$**

As  $k_o$  was increased, the rise time decreased, with a corresponding increase in the control current. Above a certain magnitude of the gain ( $k_o=1500 \text{ s}^{-1}$ ), the force response exhibited overshoot and started to include undesirable oscillations. Lower values of the gain gave sluggish responses.

Nevertheless, it is clear from Fig. 5 that the single parameter,  $k_o$ , gives a simple way of tuning the controller performance for a choice of settling times and rise times.

### Experimental Investigation of Robustness

A common concern regarding the use of model-based feedback linearizing controllers is that they could be sensitive to model parameter variations. For the system under consideration, the relevant model parameters that appear in the controller expression are the effective bulk modulus ( $\beta_e$ ), the valve coefficient ( $C_v$ ), the leakage coefficient ( $C_L$ ), and the supply ( $p_s$ ) and return ( $p_R$ ) pressures at the servovalve. The effects of the latter two parameters enter into the system dynamically due to the rather long transmission hoses used with the experimental system. In this section, experimental results are presented outlining the sensitivity of the performance of the nonlinear controller to changes in  $\beta_e$ ,  $C_v$ , and  $C_L$ . One of the parameters is changed while nominal values are kept for the other parameters in the nonlinear controller expression.

Figure 6 shows the effect of uncertainty in the effective bulk modulus ( $\beta_e$ ). The experiments were conducted by changing the effective bulk modulus by a factor of more than  $\pm 50\%$  of the nominal value of 850MPa. The lower the value of  $\beta_e$  used in the controller, the shorter the rise time, and the higher the tendency to overshoot and exhibit oscillations in the force response. On the other hand, the higher the value of  $\beta_e$  used in the controller, the more sluggish the response became. This also implies that if there were a reduction in the actual value of the effective or working bulk modulus of the oil in the system (from what was set in the controller expression), the controller performance improves or deteriorates in the manner depicted in Fig. 6. In practice, changes in the effective bulk modulus of the fluid in a hydraulic system could happen due to various reasons, such as air-entrapment (aeration), changes in mechanical compliance, and the effects of temperature.

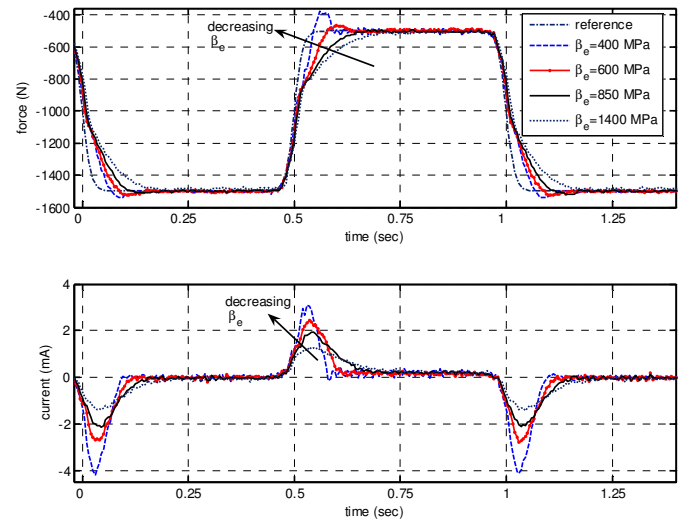


**Figure 6 Robustness to changes in the bulk modulus parameter of the nonlinear controller**

It was also observed that the system was more sensitive to decreasing changes in  $\beta_e$  than to increasing changes. The response started to overshoot with only a 25% reduction of the value of  $\beta_e$ , while the response remained virtually the same as the nominal case for a 25% increase in the value of  $\beta_e$ . The

faster responses corresponding to lower  $\beta_e$  settings also required higher current peak magnitudes, as shown in the lower plot of Fig. 6. For example, for a 25% reduction in the value of  $\beta_e$ , the current peak required was as much as 100% higher than the current peak with nominal settings for  $\beta_e$ .

Figure 7 shows the effect of uncertainty in the estimation of the valve coefficient parameter ( $C_v$ ). The experiments were conducted by changing the valve coefficient parameter by a factor of approximately  $\pm 25\%$  of the nominal value of  $2.75 \text{ cm}^3 / (\text{s.m}\sqrt{\text{MPa}})$  while keeping the other parameters at their respective nominal values. The observed trend is similar to the effect of changes in  $\beta_e$ . Here, however, the response started to show overshoot with only a 16% reduction in the value of  $C_v$ , while it remained less sensitive to increasing the value of  $C_v$  by as much as 25% of the nominal value. These observations imply that in the controller implementation, it is better to overestimate  $C_v$  and  $\beta_e$  in order to avoid overshoot and oscillations in the pressure force response.

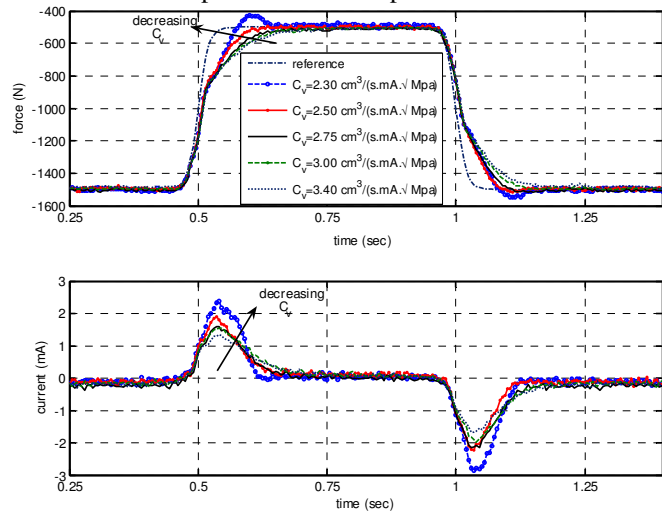


**Figure 7 Robustness to changes in the valve coefficient parameter of the nonlinear controller**

There is some asymmetry in the force responses and control current inputs for the application and removal of the step force reference corresponding to the up and down motions of the piston. These can be explained by the fact that a single value of the valve coefficient was used in the experiments for all valve ports, despite the identification data indicating a slight asymmetry, as shown in the Appendix. Furthermore, the motion of the piston is influenced by the nonlinear compliance of the neoprene rubber, which is known to exhibit hysteretic behavior.

Finally, Fig. 8 shows the effect of the leakage coefficient ( $C_L$ ) on the performance of the nonlinear controller. In these experiments, the leakage coefficients were changed by as much as 200% of the nominal value of  $0.5 \text{ cm}^3 / (\text{s.MPa})$ . This range is exaggerated, including a hypothetical negative leakage coefficient to magnify the observed response. The effect of the leakage coefficient appears to be causing offset and steady-state error when tracking the reference force. The control current does not appear to be affected significantly by changes in the settings for the leakage coefficient ( $C_L$ ) and is not repeated here. The asymmetry in the response is attributed once again to the averaging adopted for the valve coefficient and the leakage

coefficient to simplify the implementation of the nonlinear controller, as well as the hysteretic behavior of the specimen.

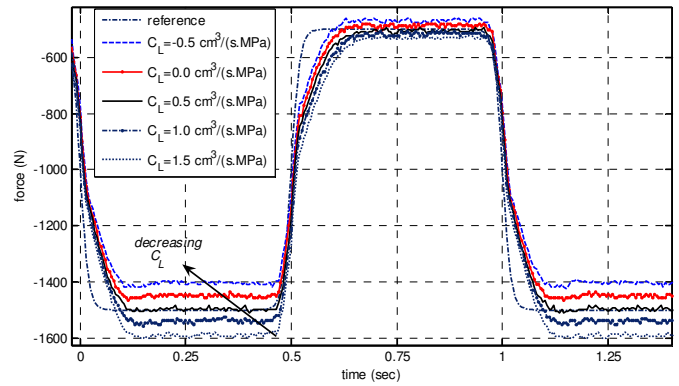


**Figure 8 Robustness to changes in the leakage coefficient parameter of the nonlinear controller**

## CONCLUSIONS

In this paper, a nonlinear force tracking controller was developed based on a near-IO linearization of a nonlinear model of an electrohydraulic actuator. This global linearization allows cancellation of the nonlinearity introduced by the valve orifice-flow, as well as the position dependent compliance in the actuator. Line effects upstream (supply) and downstream (return) of the servovalve, as well as the servovalve dynamics, were neglected for the derivation of the controller, but the controller was implemented on a realistic system subject to the presence of these neglected effects.

Experimental comparisons with standard linear controllers for tracking reference pressure force signals showed that the nonlinear control with nominal model parameters gave a compromise tracking performance between a well-tuned PID controller (for which some overshoot had to be accepted), and a sluggish linear state feedback with integral controller designed using iterative pole placement techniques on a locally linearized model of the system. Even though it may not be claimed that this comparison is exhaustive for all such systems and loading conditions, it appears that the near-IO linearizing pressure tracking controller performs better than a PID controller for well-selected gain settings. It was also shown that the nominal nonlinear controller presented in this paper can be tuned by using the single linear gain ( $k_o$ ) within limits, depending on the acceptable level of overshoot and the desired speed of response.

The robustness of the model-based nonlinear controller was also studied by conducting experiments while independently changing the controller settings for the model parameters of effective bulk modulus ( $\beta_e$ ), valve discharge coefficient ( $C_v$ ), and leakage coefficient ( $C_L$ ). It was observed that the response slowed down only slightly for as much as 25% higher than nominal settings of the  $\beta_e$  and  $C_v$  parameters. However, the response started to show overshoot and oscillation for lower settings of these parameters by about 16% for  $C_v$  and 25% for  $\beta_e$  of their respective nominal values. This implies that the nonlinear controller presented here tolerates a measurable shift in the values of these parameters without sacrificing performance. This is particularly true for the effective bulk modulus parameter whose value is generally

considered difficult to predict in a hydraulic system. Finally, the effect of changing the leakage coefficient setting in the nonlinear controller was seen to be an offset and steady-state error when tracking the smooth step reference used in the experiments.

## Appendix

Unlike the geometric parameters appearing in the control law (such as volumes and piston mass), which could be calculated fairly easily, the effective bulk modulus and the valve and leakage coefficients are not straightforward to determine for the present working status of the experimental system. Therefore, an offline "grey-box" identification technique was adopted for this work [10]. The lap parameters,  $u_1$ ,  $u_2$ ,  $u_3$ , and  $u_4$ , are neglected for this purpose. The chamber pressure state equations (1) and (2) are discretized as follows. At sampling instant  $k$ :

$$\frac{V_b + A_b x_p(k)}{\beta_b} \left( \frac{dp_b}{dt}(k) \right) = (q_b(k) + q_i(k) - A_b x_p(k)) \quad (42)$$

$$\frac{V_t - A_t x_p(k)}{\beta_t} \left( \frac{dp_t}{dt}(k) \right) = (-q_t(k) - q_i(k) + A_t x_p(k)) \quad (43)$$

Discretizing the flow rate equations (3-5) the same way and regrouping variables, the following matrix form can be written:

$$\begin{bmatrix} -(V_b + A_b x_p(k)) \left( \frac{dp_b}{dt}(k) \right) & D_1(k) & D_2(k) & (p_t(k) - p_b(k)) \end{bmatrix} \begin{bmatrix} \frac{1}{\beta_b} \\ C_{v,1} \\ C_{v,2} \\ C_{L_b} \end{bmatrix} = \begin{bmatrix} A_b \frac{dx_p}{dt}(k) \end{bmatrix} \quad (44)$$

$$\begin{bmatrix} (V_t - A_t x_p(k)) \left( \frac{dp_t}{dt}(k) \right) & D_3(k) & D_4(k) & (p_t(k) - p_b(k)) \end{bmatrix} \begin{bmatrix} \frac{1}{\beta_t} \\ C_{v,3} \\ C_{v,4} \\ C_{L_t} \end{bmatrix} = \begin{bmatrix} A_t \frac{dx_p}{dt}(k) \end{bmatrix} \quad (45)$$

where

$$D_1(k) = sg(i_v(k)) \operatorname{sgn}(p_S - p_b(k)) \sqrt{|p_S - p_b(k)|} \quad (46)$$

$$D_2(k) = sg(-i_v(k)) \operatorname{sgn}(p_b(k) - p_R) \sqrt{|p_b(k) - p_R|} \quad (47)$$

$$D_3(k) = sg(i_v(k)) \operatorname{sgn}(p_t(k) - p_R) \sqrt{|p_t(k) - p_R|} \quad (48)$$

$$D_4(k) = sg(-i_v(k)) \operatorname{sgn}(p_S - p_t(k)) \sqrt{|p_S - p_t(k)|} \quad (49)$$

For a given length  $N$  of the sampled data ( $N > 4$ ), each system of equations, (44) and (45), are linear in the unknown parameters of bulk modulus, valve coefficients, and the leakage coefficient. Each of these systems of equations has more equations than unknowns, and is therefore solved in the least squares sense, fitting the best set of parameters for the given data. In this work, several estimates from closed-loop position sine sweeps (chirp excitations) were averaged together. Furthermore, the disparate estimates of the fluid bulk modulus for the top and bottom chambers ( $\beta_t$  and  $\beta_b$ ), which take on close values in any case, were averaged together to use a single

value for the effective bulk modulus, thereby simplifying the controller expression. The same was done for the leakage coefficient and the valve coefficient. These estimates of the parameters, which are listed in Table A.1, were used as the nominal values for the control experiments in this work.

**Table A.1. Nominal Values of Controller Parameters**

Parameter	Value	Units
$\beta_e$	850	MPa
$C_{v,1}$	2.80	$cm^3 / (s.mA.\sqrt{MPa})$
$C_{v,2}$	2.73	$cm^3 / (s.mA.\sqrt{MPa})$
$C_{v,3}$	2.77	$cm^3 / (s.mA.\sqrt{MPa})$
$C_{v,4}$	2.70	$cm^3 / (s.mA.\sqrt{MPa})$
$C_L$	0.5	$cm^3 / (s.MPa)$

## REFERENCES

- Alleyne, Andrew, and Hedrick, Karl J., 1995, "Nonlinear Adaptive Control of Active Suspensions". IEEE Transactions on Control Systems Technology. **3**(1).
- Alleyne, Andrew, and Liu, Rui, 2000, "A Simplified Approach to Force Control for Electrohydraulic Systems". Control Engineering Practice. **8**: pp. 1347-1356.
- Axelson, Steve, and Kumar, K. S. P., 1988, "Dynamic Feedback Linearization of a Hydraulic Valve-Actuator Combination". in *the 1988 American Control Conference*. Atlanta, Georgia, June 15-17, 1988.
- Ayalew, Beshahwired, 2005, Nonlinear Control of Multi-Actuator Electrohydraulic Systems Based on Feedback Linearization with Application to Road Simulation, Ph D Dissertation, in Mechanical Engineering, The Pennsylvania State University
- Ayalew, Beshahwired, and Kulakowski, Bohdan T., 2005, "Modeling Supply and Return Line Dynamics for an Electrohydraulic Actuation System". ISA Transactions. **44**(2).
- Del Re, Luigi, and Isidori, Alberto, 1995, "Performance Enhancement of Nonlinear Drives by Feedback Linearization of Linear-Bilinear Cascade Models". IEEE Transactions on Controls Systems Technology. **3**(3): pp. 299-308.
- Dransfield, Peter, 1981, *Hydraulic Control Systems: Design and Analysis of their Dynamics*. Springer-Verlag.
- Hahn, H., Piepenbrink, A., and Leimbach, K.-D., 1994, "Input/Output Linearization Control of an Electro Servo-Hydraulic Actuator". in *the Third IEEE Conference on Control Applications*. Glasgow, UK.
- Hwang, C.-L., 1996, "Sliding Mode Control Using Time-varying Switching Gain and Boundary Layer for Electrohydraulic Position and Differential Pressure Control". IEEE Transactions on Control Theory Applications. **143**(4): pp. July 1996.
- Jelali, Mohieddine, and Kroll, Andreas, 2003, *Hydraulic Servo-Systems: Modelling, Identification and Control*. -(Advances in Industrial Control). London: Springer-Verlag.

11. Khalil, Hassan K., 2002, *Nonlinear Systems*. Third ed.: Prentice Hall.
12. Kugi, Andreas, 2001, *Non-linear Control Based on Physical Models*. Springer.
13. Liu, Y., and Handroos, H., 1998, "Applications of Sliding Mode Control to an Electrohydraulic Servosystem with Flexible Mechanical Load". in *the 4th International Conference on Motion and Vibration Control (MOVIC)*. Zurich, Switzerland, August 25-28, 1998.
14. Merritt, Herbert E., 1967, *Hydraulic Control Systems*. New York: John Wiley and Sons.
15. Nguyen, Q.H., Ha, Q.P., Rye, D.C, and Durrant-Whyte, H.F., 2000, "Force/Position Tracking for Electrohydraulic Systems of a Robotic Excavator". in *the 39th IEEE Conference on Decision and Control*. Sydney, Australia, December 2000.
16. Ogata, Katsuhiko, 2002, *Modern Control Engineering*. 4th ed.: Prentice Hall.
17. Plummer, A.R., and Vaughan, N.D., 1996, "Robust Adaptive Control for Hydraulic Servosystems". Transactions of ASME, Journal of Dynamic Systems, Measurement and Control. **118**: pp. 237-244.
18. Sirouspour, Mohammad R., and Salcudean, S.E., 2000, "On the Nonlinear Control of Hydraulic Servosystems". in *the IEEE International Conference on Robotics and Automation*. San Francisco, CA, April 2000.
19. Slotine, Jean-Jacques E., and Li, Wiping, 1991, *Applied Nonlinear Control*. Prentice Hall.
20. Sohl, Garret A., and Bobrow, James E., 1999, "Experiments and Simulations on the Nonlinear Control of a Hydraulic Servosystem". IEEE Transactions on Control Systems Technology. **7**(2).
21. Sun, Hong, and Chiu, George T.-C., 2001, "Motion Synchronization for Multi-Cylinder Electro-Hydraulic System". in *the 2001 IEEE/ASME International Conference on Advanced Intelligent Mechatronics*. Como, Italy, July 8-12.
22. Van Schothorst, Gerard, 1997, Modelling of Long-Stroke Hydraulic Servo-Systems for Flight Simulator Motion Control and System Design, PhD Thesis, Delft University of Technology
23. Viersma, Taco J., 1980, *Analysis, Synthesis and Design of Hydraulic Servosystems and Pipelines*. Studies in Mechanical Engineering. Vol. I. Amsterdam, The Netherlands: Elsevier Publishing Co.
24. Vossoughi, Gholamreza and Donath, Max, 1995, "Dynamic Feedback Linearization for Electrohydraulically Actuated Control Systems". Journal of Dynamic Systems, Measurement, and Control. **117**: pp. 468-477.
25. Watton, John, 1989, *Fluid Power Systems: Modelling, Simulation and Microcomputer Control*. New York: Prentice Hall.
26. Ziaei, K., and Sepheri, N., 2001, "Design of a Nonlinear Adaptive Controller for an Electrohydraulic Actuator". Journal of Dynamic Systems, Measurement and Control. **123**: pp. 449-456.